GeoHealth

RESEARCH ARTICLE
10.1029/2023GH000910

Key Points:

- Efficacy of required and best available emission control technologies tested with the GEOS-Chem model and new exposure-harm relationships
- Both reduce public exposure to particulate matter pollution and avoid 6,800 adult early deaths with legislation and 13,300 with technology
- Neither is sufficient at lessening sensitive habitat exposure to harmful loads of nitrogen and concentrations of phytotoxic ammonia

Correspondence to:
E. A. Marais,
e.marais@ucl.ac.uk

Citation:
Marais, E. A., Kelly, J. M., Vohra, K., Li, Y., Lu, G., Hina, N., & Rowe, E. C. (2023). Impact of legislated and best available emission control measures on UK particulate matter pollution, premature mortality, and nitrogen-sensitive habitats. *GeoHealth*, *7*, e2023GH000910. https://doi.org/10.1029/2023GH000910

Received 13 JUL 2023
Accepted 5 OCT 2023

Author Contributions:
Conceptualization: Eloise A. Marais
Data curation: Eloise A. Marais
Formal analysis: Eloise A. Marais, Jamie M. Kelly, Karn Vohra
Funding acquisition: Eloise A. Marais
Investigation: Eloise A. Marais, Jamie M. Kelly, Karn Vohra, Yifan Li
Methodology: Eloise A. Marais, Jamie M. Kelly, Karn Vohra, Naila Hina, Ed C. Rowe
Project Administration: Eloise A. Marais
Resources: Naila Hina, Ed C. Rowe
Software: Eloise A. Marais

Impact of Legislated and Best Available Emission Control Measures on UK Particulate Matter Pollution, Premature Mortality, and Nitrogen-Sensitive Habitats

Eloise A. Marais[1], Jamie M. Kelly[1,2], Karn Vohra[1], Yifan Li[3], Gongda Lu[1], Naila Hina[4], and Ed C. Rowe[4]

[1]Department of Geography, University College London, London, UK, [2]Now at Centre for Research and Clean Air, Helsinki, Finland, [3]Reading Academy, Nanjing University of Information Science and Technology, Nanjing, China, [4]UK Centre for Ecology & Hydrology, Environment Centre Wales, Bangor, UK

Abstract Past emission controls in the UK have substantially reduced precursor emissions of health-hazardous fine particles ($PM_{2.5}$) and nitrogen pollution detrimental to ecosystems. Still, 79% of the UK exceeds the World Health Organization (WHO) guideline for annual mean $PM_{2.5}$ of 5 μg m^{-3} and there is no enforcement of controls on agricultural sources of ammonia (NH_3). NH_3 is a phytotoxin and an increasingly large contributor to $PM_{2.5}$ and nitrogen deposited to sensitive habitats. Here we use emissions projections, the GEOS-Chem model, high-resolution data sets, and contemporary exposure-risk relationships to assess potential human and ecosystem health co-benefits in 2030 relative to the present day of adopting legislated or best available emission control measures. We estimate that present-day annual adult premature mortality attributable to exposure to $PM_{2.5}$ is 48,625 (95% confidence interval: 45,188–52,595), that harmful amounts of reactive nitrogen deposit to almost all (95%) sensitive habitat areas, and that 75% of ambient NH_3 exceeds levels safe for bryophytes and lichens. Legal measures decrease the extent of the UK above the WHO guideline to 58% and avoid 6,800 premature deaths by 2030. This improves with best available measures to 36% of the UK and 13,300 avoided deaths. Both legal and best available measures are insufficient at reducing the extent of damage of nitrogen pollution to sensitive habitats. Far more ambitious reductions in nitrogen emissions (>80%) than is achievable with best available measures (34%) are required to halve the amount of excess nitrogen deposited to sensitive habitats.

Plain Language Summary Particulate matter pollution is detrimental to human health, nitrogen pollution offsets ecosystem balance of sensitive habitats, and ammonia is toxic to plants. Here we determine the potential public health and ecosystem benefits of adopting currently legislated or best available emission control measures. We use state-of-science air quality and exposure assessment models and high-resolution data sets to estimate air pollution abundances and deposition and determine risk of human and ecosystem harm from air pollution in the UK. We find that substantial improvements to public health result from currently legislated measures, estimated as the number of avoided early deaths attributable to decline in particulate matter pollution. The number of avoided deaths doubles with best available emission control measures, as these also target particulate matter precursor emissions of ammonia from agricultural activity not mandated by existing legislation. The benefits to sensitive habitats of either legal or best available measures is near-negligible. Mitigating harm to ecosystems will require major advances in emission mitigation technologies.

1. Introduction

Air pollution is a leading risk of global premature mortality (Cohen et al., 2017; Vohra et al., 2021) and is detrimental to ecosystem balance (Phoenix et al., 2012; Sala et al., 2000). In the UK, about 29,000 adult premature deaths have been attributed to long-term exposure to ambient fine particulate matter pollution ($PM_{2.5}$) in a single year (Gowers et al., 2014) and most (70%) UK habitats with low nutrient needs are exposed to harmful levels of nitrogen (Rowe et al., 2022). Anthropogenic emissions of ammonia (NH_3), overwhelmingly (~90%) from agriculture, are a large and often dominant contributor to $PM_{2.5}$ in densely populated cities (Kelly et al., 2023; Vieno et al., 2016) and of nitrogen deposited to ecosystems (Tomlinson et al., 2021). NH_3 is also a phytotoxin (Dise et al., 2011; Krupa, 2003; van Herk et al., 2007).

Supervision: Eloise A. Marais, Gongda Lu
Validation: Eloise A. Marais, Jamie M. Kelly, Yifan Li, Gongda Lu
Visualization: Eloise A. Marais, Gongda Lu
Writing – original draft: Eloise A. Marais
Writing – review & editing: Jamie M. Kelly, Karn Vohra, Yifan Li, Gongda Lu, Naila Hina, Ed C. Rowe

Measures to reduce NH_3 emissions from agricultural activity in the UK are limited to voluntary implementation of documented best practices (DEFRA, 2018). Over the past 3 decades (1990–2020) anthropogenic NH_3 emissions have declined by just 0.6% a^{-1}; much slower than decline in other $PM_{2.5}$ precursors such as sulfur dioxide (SO_2) at 3.0% a^{-1} and nitrogen oxides (NO_x) at 2.4% a^{-1} (Churchill et al., 2022). NH_3 is a semi-volatile, alkaline gas that partitions reversibly to acidic aerosols forming ammonium (NH_4). Due to sustained controls on local and national SO_2 and NO_x sources, concentrations of acidic sulfate aerosols formed from SO_2 oxidation and acidic nitrate aerosols formed from NO_x oxidation have declined, contributing to decline in NH_4 (Tang et al., 2018). Weakening of the NH_3 aerosol sink and absent controls on agriculture have caused an increase in ambient NH_3 concentrations and the amount of NH_3 deposited to terrestrial ecosystems via dry and wet deposition (Hertel et al., 2012). This is detrimental to habitats sensitive to excessive nitrogen loads, as it causes loss of plant species that are out-competed by nitrogen-tolerant plants and reduces resilience to environmental stressors such as drought (Bobbink et al., 1998). Lichens and bryophytes, prevalent classes of plants in the UK, are also harmed by exposure to ambient NH_3. The increased nitrogen and alkalinity from NH_3 alters species composition by favoring nitrophytes and decreasing abundance of acidophytes (Sutton et al., 2020). This shift has been observed to occur from ~1 μg m^{-3} at field sites across Europe (Cape et al., 2009).

The UK commits to sustained decline in air pollutant precursor emissions as a signatory of the United Nations Economic Commission for Europe (UNECE) Convention on Long-Range Transboundary Air Pollution (CLRTAP) legislated through the UK National Emission Ceilings Regulations (UK, 2018). The UK met the 2020 targets, according to bottom-up estimates from the National Atmospheric Emission Inventory (NAEI) (Richmond et al., 2020), though top-down NH_3 emissions estimated with satellite observations suggest the NAEI may underestimate NH_3 emissions by 30%–50% (Marais et al., 2021). NH_3 emissions targets, reported as percent reduction relative to 2005, are 8% in any year in 2020–2029 and 16% from 2030; modest in comparison to SO_2 (59% in 2020–2029 and 79% from 2030) and NO_x (42% in 2020–2029 and 63% from 2030) (Office of the European Union, 2016a). Readily available emission control measures targeting the largest agricultural sources of NH_3, fertilizer use and livestock and manure management (Churchill et al., 2022), offer efficacies that range from 10% to 20% decrease in emissions for switching to low nitrogen feed, to 80% decrease by fitting scrubbers to animal housing, to up to 93% by phasing out urea-based fertilizers (Klimont & Brink, 2004).

Past studies that have assessed separately the public health and ecosystem benefits of emissions controls suggest current measures offer greater benefits to public health than the expense to implement (Giannakis et al., 2019), and that mitigating harm of ecosystem exposure to excess nitrogen would require large (at least 40%) reductions in NH_3 emissions (Woodward et al., 2022). Here we investigate whether adoption of measures to meet current legislation or of readily available maximum technically feasible technologies across all sectors, including agriculture, are sufficient to offer combined benefits to public health and to habitats harmed by exposure to NH_3 and excess nitrogen deposition in the UK. We do this by implementing emissions scenarios from the EU's Evaluating the Climate and Air Quality Impacts of Short-Lived Pollutants (ECLIPSE) project (Stohl et al., 2015) in the GEOS-Chem model to simulate the response of ambient $PM_{2.5}$ and NH_3 and nitrogen deposition to emissions changes. We apply these to high spatial resolution data sets of contemporary nitrogen deposition to sensitive habitats and models of the relationship between exposure and risk of harm to calculate adult premature mortality in each UK administrative area and the scale of harm of habitat exposure to nitrogen deposition and ambient NH_3.

2. Materials and Methods

2.1. GEOS-Chem Model Description

We use the GEOS-Chem chemical transport model (CTM) version 13.0.0 (https://doi.org/10.5281/zenodo.4618180; accessed 12 December 2021) to simulate present-day and future UK surface concentrations of $PM_{2.5}$ and NH_3 and total (wet and dry) nitrogen deposition due to emissions controls adopted across Europe. The future scenarios are representative of emissions likely in 2030 from adopting either (a) currently legislated emission controls or (b) maximum technically feasible measures. In what follows, the scenarios and associated model results are labeled "PD" for the present-day simulation in 2019, "CLE" for adopting measures to meet current legislation by 2030 and "MTF," also for 2030, but following adoption of maximum technically feasible measures. The model is nested over the UK (49.25°N–59.50°N, 9.375°W–3.75°E) at 0.25° × 0.3125° (28 km latitude × 20 km longitude at the center of the domain) and is updated 3-hourly with boundary conditions from a global GEOS-Chem simulation at 4° × 5°. The model uses GEOS-FP assimilated meteorology from the NASA

Global Modeling and Assimilation Office. All simulations are driven with meteorology for the same year (2019) to isolate the effect of changes in anthropogenic emissions only. The year 2019 instead of 2020 is chosen for the PD simulation, as it is unaffected by the brief, but dramatic decline in emissions resulting from lockdown measures in the first wave of the COVID-19 pandemic in Spring 2020 (Potts et al., 2021).

Anthropogenic emissions in the PD simulation are mostly consistent with those detailed in Kelly et al. (2023) from an earlier model version (v12.1.0) for the same year (2019) used to characterize sources contributing to $PM_{2.5}$ in UK cities. These emissions are from the NAEI for the UK and the European Monitoring and Evaluation Program (EMEP) for all other European countries. Emissions scaling is applied to terrestrial NAEI and EMEP SO_2 emissions to address a positive bias in modeled SO_2 surface concentrations (Marais et al., 2021) and to NAEI and EMEP NH_3 emissions to resolve differences between bottom-up emissions and those derived with satellite observations of NH_3 column densities (Marais et al., 2021). The scale factors applied are a uniform 60% decrease in land-based SO_2 emissions and 50% increase in NH_3 emissions. The NH_3 emissions scaling is supported by agreement between the model and surface observations of NH_4 concentrations at rural sites throughout the UK with this scaling (Kelly et al., 2023) and, as we show in this work, modeled and observed rainwater concentrations of reduced ($NH_x \equiv NH_3 + NH_4$) nitrogen.

For the future (2030) scenario simulations, we scale anthropogenic emissions in all countries in Europe in the PD simulation using projected changes in emissions derived from integrated assessment models. All anthropogenic emissions, except aviation, are from the ECLIPSE project (Stohl et al., 2015). Emissions due to control measures are predicted in 5-year intervals from 1990 to 2050 for multiple major pollutants and precursors (SO_2, NO_x, NH_3, primary $PM_{2.5}$, non-methane volatile organic compounds (NMVOCs), and carbon monoxide) and sectors (agriculture, residential, commercial, energy, industry, on- and off-road transport, shipping, and waste). We use data from the latest version of ECLIPSE (v6b; https://previous.iiasa.ac.at/web/home/research/researchPrograms/air/ECLIPSEv6b.html; last accessed 3 August 2022). For the CLE simulation, we use the ECLIPSEv6b "CLE" scenario, as this incorporates changes in anthropogenic emissions due to implementation of mitigation measures legislated as recently as 2018. For the MTF simulation, we use the ECLIPSEv6b "MTFR" scenario that assumes adoption of all available air pollution control measures. The ECLIPSEv6b shipping emissions were recently revised to capture a wider range of emission factors for primary particles. Only the CLE emissions were updated, so the same shipping emissions are used for CLE and MTF scenarios. ECLIPSEv6b does not predict aviation emissions, so we take these from Intergovernmental Panel on Climate Change (IPCC) projections downloaded using the Representative Concentration Pathways Database tool version 2.0.5 (https://tntcat.iiasa.ac.at/RcpDb/; last accessed 3 August 2022). The IPCC emissions we use are the business-as-usual Shared Socioeconomic Pathways (SSP) 2–4.5 (Fricko et al., 2017) for the CLE scenario and the sustainable pathways SSP 1–2.6 (van Vuuren et al., 2017) for the MTF scenario. All emissions data are provided as gridded annual values at $0.5° \times 0.5°$, so we derive annual scale factors to apply to PD emissions at $0.5° \times 0.5°$ resolution. Hourly, monthly and seasonal scaling factors are the same as those used for the PD emissions. The Harmonized Emission Component (HEMCO) processing package (Keller et al., 2014) is used to apply scaling factors and to grid emissions to the GEOS-Chem boundary condition and nested model resolutions.

Natural emissions are the same for all scenarios. These are $0.25° \times 0.3125°$ offline emissions of hourly dust (Meng et al., 2021), biogenic VOCs (Weng et al., 2020), and soil NO_x (Weng et al., 2020), and 3-hourly lightning NO_x (Murray et al., 2012). Natural NH_3 emissions are monthly values from the Global Emissions InitAtive (GEIA) inventory for oceans and soils (Bouwman et al., 1997) and annual values from Riddick et al. (2012) for seabirds. GEIA NH_3 emissions are halved to address a known overestimate in these (Paulot et al., 2014).

GEOS-Chem simulates the individual $PM_{2.5}$ components sulfate, nitrate, NH_4, primary and secondary organic aerosols (POA, SOA), black carbon (BC), sea salt, and dust. Formation of sulfate from oxidation of SO_2, detailed in Park et al. (2004), is dominated by in-cloud oxidation by hydrogen peroxide. Formation of aerosol nitrate from uptake of nitric acid (HNO_3) and aerosol NH_4 from reversible partitioning of NH_3 is determined with the thermodynamic equilibrium model ISORROPIA-II (Fountoukis & Nenes, 2007). SOA is estimated with fixed mass yields applied to anthropogenic and biogenic NMVOCs emissions (Pai et al., 2020).

Model representation of other $PM_{2.5}$ components are detailed in Jaeglé et al. (2011) for sea salt and Fairlie et al. (2007) for dust. The proportion of BC and POA emitted as hydrophobic (80% for BC, 50% for POA) ages to hydrophilic at an e-folding time of 1.15 days (Chin et al., 2002; Cooke et al., 1999). Dry deposition is via the Wesely (1989) resistance-in-series scheme. Wet deposition includes scavenging in convective updrafts and

rainfall, as well as washout, entrainment and detrainment as detailed in Liu et al. (2001) for water-soluble aerosols and Amos et al. (2012) for gases. We enable the fast scavenging mechanism of Luo et al. (2020) that addresses a positive cold season bias in modeled surface concentrations of aerosol nitrate and NH_4 across Europe. Chemical initialization of the model is achieved with spin-ups of a year for global boundary conditions and 2 months for the PD, CLE, and MTF nested domain simulations.

The model is sampled from 1 January to 31 December 2019 to calculate annual mean surface concentrations of NH_3 and components of $PM_{2.5}$ and of reduced and oxidized gas and aerosol-phase nitrogen wet and dry deposition fluxes. Surface concentrations of $PM_{2.5}$ are calculated at standard conditions of temperature (20°C) and pressure (1 atm) and associated aerosol water is determined using hygroscopic growth factors of individual $PM_{2.5}$ components representative of 50% relative humidity, as detailed in Kelly et al. (2023). Total nitrogen deposition is calculated as the sum of GEOS-Chem deposition fluxes of reduced and oxidized nitrogen compounds that wet and dry deposit (NH_3, NH_4, HNO_3, aerosol nitrates, peroxy acetyl nitrates, and gas-phase organonitrates) and that only dry deposit (NO_2, dinitrogen pentoxide, and C1-C3 alkylnitrates).

2.2. Surface Observations for GEOS-Chem Evaluation

Kelly et al. (2023) compared UK network measurements of $PM_{2.5}$ to $PM_{2.5}$ obtained with an earlier version of the model driven with similar PD emissions to those detailed in Section 2.1. In that comparison, GEOS-Chem annual mean $PM_{2.5}$ is spatially consistent with the annual mean of the observations ($R = 0.66$), but with an expected model underestimate (of 11%), as many of the network sites are in cities along busy roads. We compare our PD model output to that of Kelly et al. (2023) archived on the University College London Data Repository (Marais et al., 2022).

We also evaluate model simulation of nitrogen wet deposition with surface network rainwater concentrations of oxidized and reduced nitrogen. These are from rural and semi-rural UK Eutrophying and Acidifying Pollutants (UKEAP) Precipitation Network (Precip-Net) measurement sites established to determine long-term trends in wet deposition of air pollutants. Data at the 41 sites operational in 2019 are from the UK-Air data portal (https://uk-air.defra.gov.uk/data/data_selector; last accessed 15 March 2023). Samples at these sites are collected every 2 weeks to record rainwater volume and measure oxidized (nitrate) and reduced (NH_x) nitrogen rainwater concentrations (Kelleghan et al., 2021). We identify and remove observations contaminated by bird strikes (Conolly et al., 2021) and correct biases in GEOS-FP monthly total precipitation (Neelam et al., 2021; Paulot et al., 2014; Travis et al., 2016). Only three samples are contaminated with bird strikes, identified with phosphate (P) rainwater concentrations >0.1 mg P L^{-1}. We correct for biases in GEOS-FP precipitation by multiplying GEOS-FP monthly total precipitation (precip) by the correction factor derived by Paulot et al. (2014) ($[\text{precip}_{\text{observed}}/\text{precip}_{\text{modeled}}]^{0.6}$), where modeled precipitation is for grids coincident with UKEAP sites. We use the corrected modeled rainwater volume and GEOS-Chem wet deposition fluxes to calculate GEOS-Chem nitrate and NH_x rainwater concentrations.

2.3. Public Health Burden Attributable to Exposure to $PM_{2.5}$

We use the hybrid health risk assessment model from Weichenthal et al. (2022) to calculate adult premature deaths attributable to exposure to $PM_{2.5}$ in the PD and by 2030 due to CLE and MTF control measures. The hybrid model merges two functions to represent the relationship between $PM_{2.5}$ and relative risk (RR) of all-cause adult (25+ years) premature mortality covering a wide $PM_{2.5}$ concentration range. The functions are known as the extended Shape Constrained Health Impact Function (eSCHIF) and Fusion. eSCHIF was derived with Canadian Census Health and Environment Cohort (CanCHEC) study data covering 2.5–17.7 μg m^{-3} (Brauer et al., 2022; Weichenthal et al., 2022). Fusion itself is a hybrid of three widely used health-risk assessment models, established to address deficiencies in each (Burnett et al., 2022). As the Fusion function is underconstrained at very low $PM_{2.5}$ concentrations, Weichenthal et al. (2022) used eSCHIF at 2.5–5 μg m^{-3}, choosing the recently revised World Health Organization (WHO) guideline value of 5 μg m^{-3} (WHO, 2021) to transition between the two curves. This requires an artificial ~14% increase in Fusion RRs at concentrations relevant to the UK to achieve a continuous curve. We avoid this by rather adapting the code provided by Weichenthal et al. (2022) to transition at the intersection of the two curves at 9.8 μg m^{-3}.

The eSCHIF RR function we apply from 2.5 to 9.8 μg m^{-3} is:

$$\text{eSCHIF}(z) = \exp\left\{\frac{\phi \ln\left(\frac{z-z_{\text{cf}}}{\alpha}+1\right)}{\left(1+\exp\left(-\frac{z-z_{\text{cf}}-\tau}{\upsilon}\right)\right)} + \omega \ln\left(\frac{(z-z_{\text{cf}})}{\delta}+1\right)\right\} \quad (1)$$

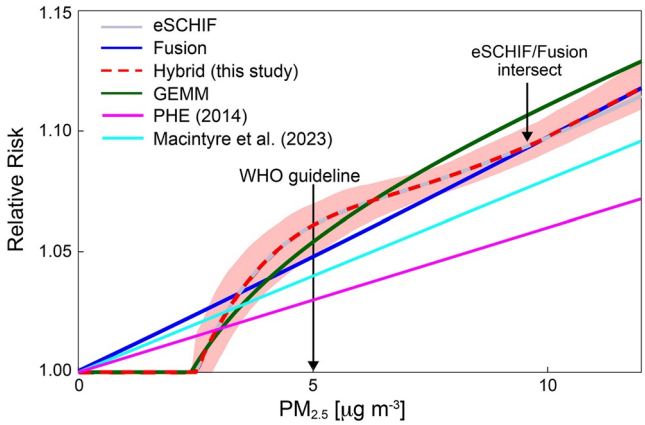

Figure 1. Curves relating relative risk of adult premature mortality to ambient $PM_{2.5}$. Lines are eSCHIF (Equation 1, gray), Fusion (Equation 2, blue), the hybrid of the two (red dashed), the Global Exposure Mortality Model (GEMM, green), and curves used in past UK studies by Public Health England (PHE, 2014) (magenta) and Macintyre et al. (2023) (cyan). Red shading is the hybrid curve 95% confidence interval. Arrows point to the WHO, 2021 guideline at 5 μg m^{-3} and the intersection of eSCHIF and Fusion at 9.8 μg m^{-3}.

where z is annual mean $PM_{2.5}$, z_{cf} is the counterfactual concentration of 2.5 μg m^{-3} at and below which RR = 1, and $\phi,\alpha,\tau,\upsilon,\omega$ and δ are best-fit parameters derived from the cohort data. The Fusion curve we apply for $PM_{2.5} > 9.8$ μg m^{-3} is:

$$\text{Fusion}(z) = \exp\left\{\gamma \times (\min(z,\mu) + \int_{\mu}^{z}\left(1 + \frac{1-\rho}{\rho}\left(\frac{x-\mu}{\theta-\mu}\right)^{\frac{\theta-\mu}{\theta(1-\rho)}}\right)^{-1} dx + \rho\theta \ln(\max(z,\theta)/\theta)\right\} \quad (2)$$

where $\gamma,\mu,\rho,$ and θ are best-fit parameters obtained with the cohort data. $PM_{2.5}$ (z) in Equations 1 and 2 are PD, CLE and MTF annual means in each GEOS-Chem grid.

Figure 1 shows the shapes of the Fusion and eSCHIF curves and the hybrid of the two for $PM_{2.5} \leq 12$ μg m^{-3}, the peak measured and modeled annual mean $PM_{2.5}$ in the UK in 2019 (Kelly et al., 2023). Fusion is linear at the range relevant to the UK. eSCHIF is supralinear from 2.5 to ~5 μg m^{-3}; a shape supported by epidemiological cohort studies conducted in Europe and North America (Di et al., 2017; Strak et al., 2021).

The RR values obtained with Equations 1 and 2 are used to calculate the fraction of adult nonaccidental deaths attributable to exposure to $PM_{2.5}$, the attributable fraction (AF):

$$\text{AF} = \begin{cases} 1 - \frac{1}{\text{eSCHIF}(z)} & 2.5\ \mu\text{g m}^{-3} < z \leq 9.8\ \mu\text{g m}^{-3} \\ 1 - \frac{1}{\text{FUSION}(z)} & z > 9.8\ \mu\text{g m}^{-3} \end{cases} \quad (3)$$

These are calculated for each GEOS-Chem grid and further used to estimate adult excess deaths attributable to exposure to $PM_{2.5}$ as the product of AF, adult population, and baseline nonaccidental mortality rates (BMR):

$$PM_{2.5}\text{ excess deaths} = \text{AF} \times \text{Adult Population} \times \text{BMR} \quad (4)$$

Adult population and BMRs are for 2019 throughout to avoid influence from COVID in 2020 and uncertainties predicting total population and demographics out to 2030. BMRs are from the Global Burden of Disease (GBD) provided in 5-year age increments (https://vizhub.healthdata.org/gbd-results/; last accessed 30 March 2023), where the nonaccidental premature deaths we use are the sum of non-communicable diseases and lower-respiratory infections for adults 25 years and older. These account for 96% of UK total adult premature deaths. BMRs are reported for each administrative area in England and at the national scale for Scotland, Wales and Northern Ireland. UK population data reported in 5-year age increments at 30 arc-seconds (~1 km) resolution are from WorldPop (https://dx.doi.org/10.5258/SOTON/WP00671; last accessed 5 August 2022). The GBD BMRs and cumulative WorldPop data for age-groups 25 years and older are gridded to the GEOS-Chem grid to collocate population and $PM_{2.5}$ pollution hotspots. These gridded data of AFs, adult population and BMRs are multiplied (Equation 4) and the resultant gridded excess deaths are sampled with shapefiles of UK administrative areas (county councils, unitary authorities and metropolitan counties) from the Database of Global Administrative Areas (GADM) (https://gadm.org/; last accessed 17 March 2023). This yields excess deaths in all 184 administrative areas: 119 in England, 32 in Scotland, 22 in Wales, and 11 in Northern Ireland. Premature mortality estimates are reported with 95% confidence using uncertainties in RR only. The 95% confidence interval (CI) for the hybrid curve is shown in Figure 1.

We test sensitivity of premature mortality estimates to health-risk assessment model choice by comparing to values obtained with the Global Exposure Mortality Model (GEMM) (Burnett et al., 2018). The GEMM curve, included in Figure 1, is the version obtained without the Chinese Male Cohort, as detailed in Burnett et al. (2018). GEMM is also for adults 25 years and older and has the same counterfactual $PM_{2.5}$ as the hybrid model (RR = 1 at 2.5 μg m^{-3}). GEMM RRs are less than the hybrid model at $PM_{2.5} < 7$ μg m^{-3} and exceed the hybrid model above this.

Table 1
Nitrogen Critical Loads Applied to Sensitive Habitats in the UK

Sensitive habitat	Critical load (kg N ha^{-1} a^{-1})[a]	UK coverage (km^2)	Contribution (%)[b]
Acid grasslands	6	20,342	22
Bog	5	8,514	9
Dwarf shrub heath	5	21,496	23
Calcareous grasslands	10	1,012	1
Coniferous woodland	10	14,452	16
Dune grassland	5	631	<1
Deciduous woodland	10	8,706	9
Unmanaged Beech (Fagus) woodland	10	2,059	2
Montane	5	4,915	5
Unmanaged oak woodland	10	6,958	7
Salt marsh	10	808	<1
Unmanaged Scotts pine woodland	5	1,485	1
Unmanaged other woodland	10	1,423	2

[a]Lower end of the range of recently updated values from Rowe and Hina (2023) to represent the threshold value above which harm occurs. [b]Percent contribution to UK sensitive area total coverage of 92,801 km^2.

2.4. Harm to Nitrogen Sensitive Habitats

We assess the efficacy of emission control scenarios at alleviating harm to nitrogen-sensitive habitats by quantifying the change in the amount and extent of nitrogen deposited in excess of critical loads and the extent of ambient $NH_3 > 1$ μg m^{-3} indicative of harm to bryophytes and lichens. Table 1 lists the UK habitats sensitive to nitrogen deposition and the recommended critical loads of each of these habitats. These range from 5 kg nitrogen (N) ha^{-1} a^{-1} for low resilience habitats such as bogs and montane habitats to 10 kg N ha^{-1} a^{-1} for more resilient habitats such as calcareous grasslands and all woodlands except Scotts pine. The critical loads we use have been recently revised (Bobbink et al., 2022) and are 2–7 kg N ha^{-1} a^{-1} less than previously recommended values compiled by Hall et al. (2015) for all sensitive habitats except the unmanaged oak and other woodlands habitats that are unchanged. We average the critical loads in Table 1 onto the GEOS-Chem grid using maps of fractional coverage of sensitive habitats provided at 1 km resolution by the UK Centre for Ecology and Hydrology (UKCEH). These gridded critical loads are shown in Figure 2a. Nitrogen sensitive habitats account for 38% of UK land area, dominated by acid grasslands, dwarf shrub heath and coniferous woodlands. The other 62% is mostly arable land and fertilized grasses. Most (58%) of the nitrogen sensitive areas are in Scotland (Rowe et al., 2022). The total coverage in Table 1 of 92,801 km^2 is 973 km^2 less than is in the critical loads trends report compiled by the UKCEH (Rowe et al., 2022), as the GEOS-Chem UK nested domain excludes Shetland Islands.

GEOS-Chem is too coarse to resolve deposition to individual sensitive habitats. This is particularly apparent across southern and central England where sensitive habitats account for <20% of GEOS-Chem grid areas (Figure 2b). GEOS-Chem wet deposition also does not account for enhanced nitrogen washout from orographic lifting over upland areas (Dore et al., 1992; Fowler et al., 1988). Given this, we use UKCEH Concentration Based Estimated Deposition (CBED) annual multiyear (2018–2020) mean nitrogen deposition rates provided at 5 km resolution to calculate PD nitrogen deposition exceedances. The derivation of this data set is detailed in Rowe et al. (2022). Briefly, CBED wet deposition fluxes are determined with UK Met Office annual precipitation data and monitoring network observations of ambient reactive nitrogen concentrations and rainwater ion concentrations interpolated to the 5 km CBED grid and by accounting for enhanced wet deposition due to orographic lifting and deposition of cloud droplets to vegetation. Dry deposition is determined with a resistance-in-series model using NH_3 concentrations simulated by the EMEP regional CTM at 5 km resolution and vegetation-specific deposition velocities. The CBED deposition data provides nitrogen deposition values for forests and open vegetation. Deposition rates to forests are ∼60% more than values for open vegetation, due to greater surface area of forest vegetation. We map CBED deposition data to the GEOS-Chem grid using UKCEH habitat maps of the spatial coverage of the six woodlands and seven open vegetation habitats in Table 1 before using the gridded deposition

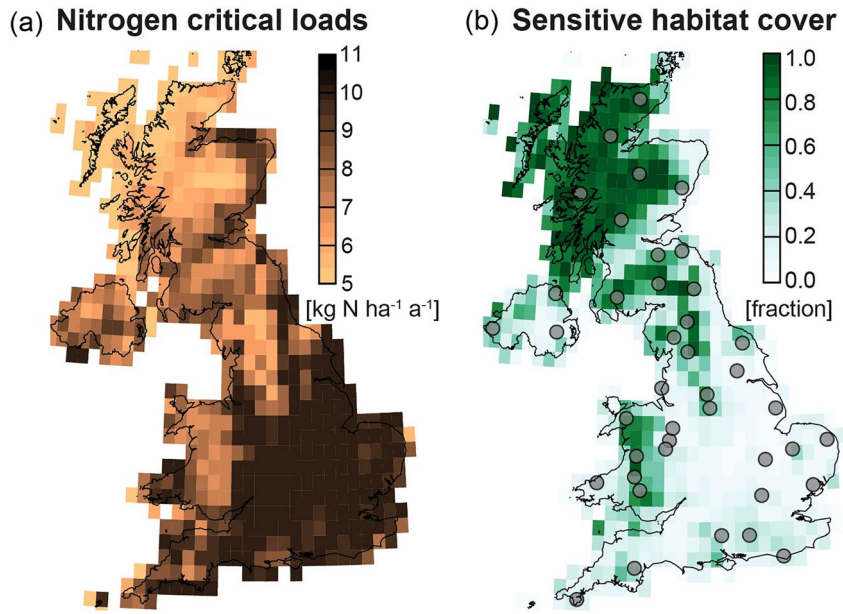

Figure 2. UK nitrogen sensitive habitat critical loads and coverage on the GEOS-Chem grid. Maps are sensitive habitat nitrogen critical loads in kg N (ha sensitive habitat)$^{-1}$ a^{-1} (a) and fractional cover of sensitive habitats in each GEOS-Chem gridcell. Gray circles in (b) are UKEAP Precip-Net monitoring site locations (Section 2.2).

data to calculate nitrogen exceedances for the PD. This yields maps of nitrogen deposition in kg N (ha sensitive habitat)$^{-1}$ a^{-1}. We then use GEOS-Chem PD, CLE and MTF total nitrogen deposition to calculate changes in nitrogen deposition to quantify the effect of CLE and MTF emission controls on risk of harm to sensitive habitats.

3. Results and Discussion

3.1. Emission Control Scenarios and GEOS-Chem Evaluation

Figure 3 shows annual anthropogenic emissions of NH_3, NO_x, SO_2, and primary $PM_{2.5}$ used in GEOS-Chem PD and future (CLE, MTF) simulations. These are totals for the NAEI domain, so include shipping emissions in UK territorial waters. PD emissions total 452 Gg NH_3, 712 Gg NO_x as NO, 45 Gg SO_2 as S, and 102 Gg primary $PM_{2.5}$. Agriculture accounts for ~90% of anthropogenic NH_3, dominated by fertilizer use and livestock and manure management. NO_x is mostly from land transport and shipping and is the only $PM_{2.5}$ precursor with non-negligible contribution from aviation of 5% in the PD. SO_2 is mostly from industrial processes, energy generation and shipping (Churchill et al., 2022). Primary $PM_{2.5}$ is mostly from residential and commercial sectors and industry.

All air pollutant precursors except NH_3 decline in the CLE scenario by 14% for SO_2, 34% for NO_x, and 24% for primary $PM_{2.5}$. According to ECLIPSEv6b emissions projections, the UK fails to meet its CLRTAP emissions ceilings commitment of 8% decrease in NH_3 emissions with current measures. If instead maximum technically feasible measures are adopted, NH_3 declines by 19%. This results from measures such as low nitrogen livestock feed, covered manure storage, low emissions manure spreading methods, filters and scrubbers of air ventilated from animal housing, and low NH_3 alternatives to urea-based fertilizers (Backes et al., 2016). The 19% decrease is still less than half the minimum decline that Woodward et al. (2022) estimate is needed to significantly mitigate harm to sensitive habitats using less strict critical loads than the updated recommended values in Table 1. The 2% increase in CLE NH_3 emissions in Figure 3a is due to limited adoption of suggested measures to offset increase in NH_3 emissions from intensification of agriculture to meet growing food and market demands (Alexandratos & Bruinsma, 2012). NO_x emissions from shipping for both the CLE and MTF scenarios decrease by 21% due to NO_x emissions regulations adopted in the Baltic and North Seas since 2021 (IMO, 2019). Shipping emissions of SO_2 increase by 12% relative to the PD, increasing its contribution to anthropogenic SO_2 emissions from 29% for the PD to 38% for the CLE and 54% for the MTF. According to ECLIPSEv6b, large (>70%) reductions in ship emissions of SO_2 from switching to low-sulfur fuel occur a decade earlier in 2010–2020 (Office of

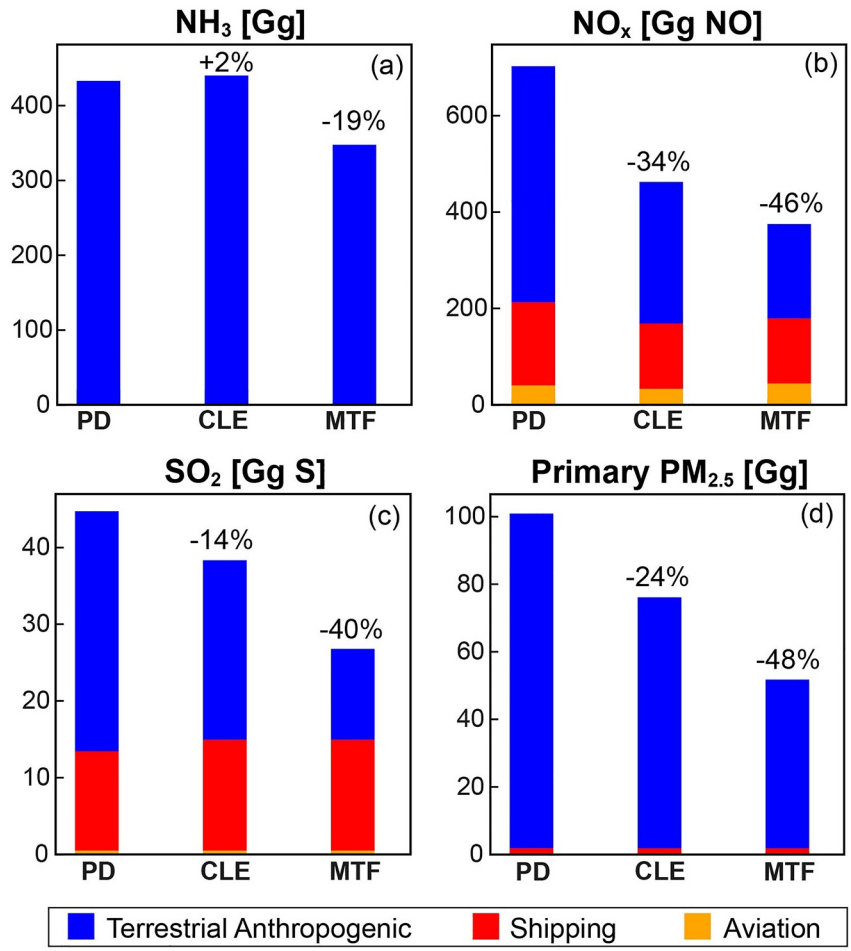

Figure 3. UK present and future anthropogenic emissions of $PM_{2.5}$ and nitrogen pollution precursors. Panels show total annual emissions of NH_3 (a), NO_x (b), SO_2 (c), and primary $PM_{2.5}$ (d) for PD and future (2030) CLE and MTF emissions scenarios. Primary $PM_{2.5}$ is the sum of BC, POA and dust. Inset values are percent change in CLE and MTF relative to PD. Bar colors distinguish surface-bound terrestrial anthropogenic sources (blue), ships (red), and aircraft (yellow).

the European Union, 2016b). Aviation NO_x decreases by 19% in the CLE scenario and increases by 10% in the MTF scenario, due to trade-offs between emissions of NO_x and the greenhouse gas carbon dioxide (Freeman et al., 2018; Skowron et al., 2021). The relative contribution of aviation to total NO_x emissions is 7% for CLE and 11% for MTF. Steep decline in terrestrial anthropogenic NO_x, SO_2 and primary $PM_{2.5}$ in the MTF scenario results from a combination of flue gas desulfurization and very efficient dedusters applied to power plants and industrial sources, improved domestic stoves and burning technology, and faster adoption of stricter Euro standards for vehicles (Henneman et al., 2016).

Figure 4a shows GEOS-Chem PD annual mean $PM_{2.5}$. Grids have the same spatial distribution ($R = 0.99$) and average only 6% or 0.4 μg m^{-3} more than is simulated with the model version from Kelly et al. (2023) (Section 2.2). Monthly UK mean $PM_{2.5}$ in this work ranges from 0.6 μg m^{-3} less (February) to 1.9 μg m^{-3} more (April) than is obtained by Kelly et al. (2023). These differences are due to more efficient cold season wet deposition of nitrate and NH_4 and less extreme downscaling of SO_2 emissions in this work. The latter enhances formation of springtime inorganic sulfate, nitrate and ammonium aerosol. As in Kelly et al. (2023), 79% of GEOS-Chem grids in Figure 4a exceed the WHO, 2021 annual mean $PM_{2.5}$ guideline of 5 μg m^{-3}.

Figure 5 compares observed and modeled rainwater concentrations of nitrate and NH_x to assess GEOS-Chem PD nitrogen wet deposition at UKEAP monitoring sites (Figure 2b). Temporal coverage at all sites exceeds 75%. Site mean UKEAP rainwater concentrations are 0.34 mg N L^{-1} for nitrate and 0.42 mg N L^{-1} for NH_x. The correction applied to GEOS-FP total precipitation (Section 2.2) leads to changes in GEOS-FP rainwater volume that varies

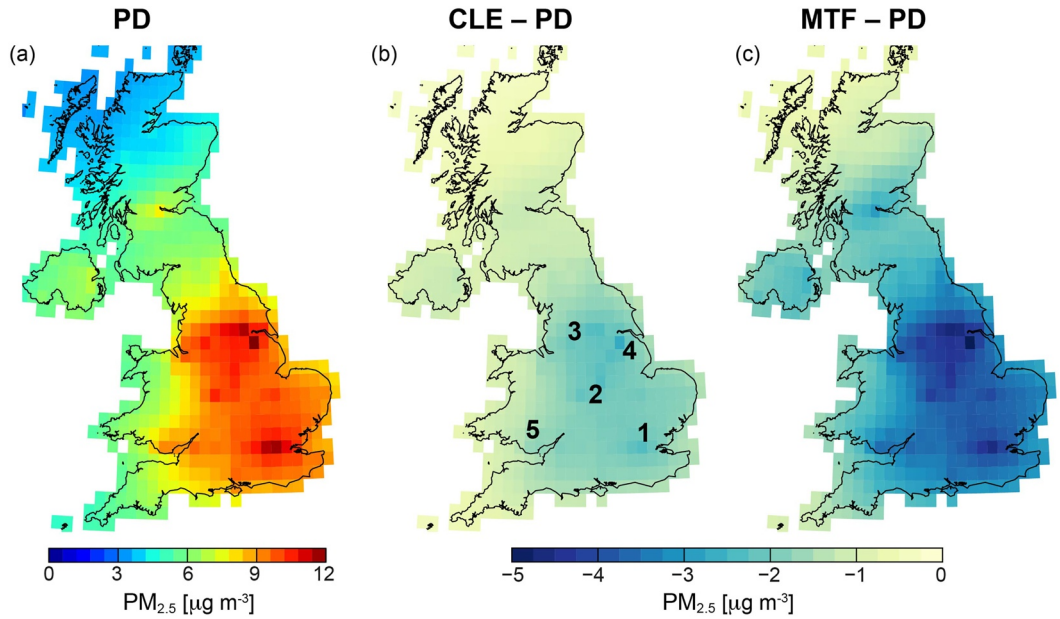

Figure 4. Effect of emission control measures on UK $PM_{2.5}$. Maps are GEOS-Chem annual mean $PM_{2.5}$ in 2019 (PD) (a) and changes in $PM_{2.5}$ relative to the PD due to controls on anthropogenic sources to meet current legislation (CLE minus PD) (b) and adoption of readily available maximum technically feasible measures (MTF minus PD) (c). Inset numbers in (b) are locations with greatest decline in $PM_{2.5}$ discussed in the text: 1. London, 2. Birmingham, 3. Manchester and Leeds, 4. East Yorkshire, and 5. South coast of Wales.

from a 40%–50% increase in December and January, to a 23%–26% decrease in April and July, to near-negligible (4%–6%) difference in March and November. The overall effect on total rainwater volume in 2019 is a small 4% increase. Without the correction, the correlation between modeled and observed NH_x is weak ($R = 0.47$) and there is an apparent underestimate in the model of 33% for nitrate and 22% for NH_x. With the rainwater volume correction, both nitrate ($R = 0.85$) and NH_x ($R = 0.64$) are spatially consistent, modeled nitrate is 15% or 0.05 mg N L^{-1} less than is observed, and modeled and observed NH_x are equivalent. A 15% difference in oxidized NO_x is more than the prescribed 8% error in NAEI NO_x emissions (Richmond et al., 2020), but in agreement with a low bias in NAEI NO_x emissions when compared to top-down emissions derived with satellite observations of tropospheric columns of nitrogen dioxide (NO_2) (Pope et al., 2022).

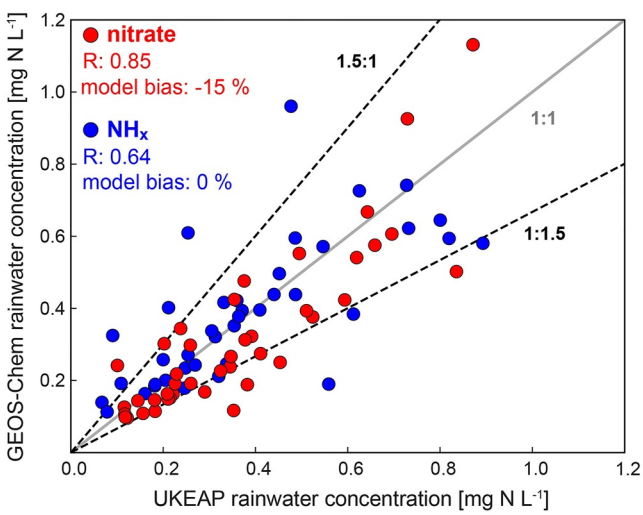

Figure 5. Evaluation of modeled nitrogen wet deposition. Scatterplot compares observed (UKEAP) and modeled (GEOS-Chem) rainwater concentrations of oxidized (nitrate, red) and reduced (NH_x, blue) nitrogen at UKEAP sites in 2019. The gray line is the 1:1 relationship and the black dashed lines bound the 50% difference. Numbers inset are the Pearson's correlation coefficient (R) and the model normalized mean bias. Site locations are in Figure 2(b).

The contribution of wet deposition to total nitrogen deposition is 58% for grids coincident with UKEAP sites. Many of these sites evaluate model grids dominated by sensitive areas, particularly in Scotland (Figure 2b). The 58% contribution to total deposition is similar (57%) for all UK grids and includes contributions from NH_3 (31%), HNO_3 (28%), NH_4 (25%) and aerosol nitrate (15%). The 42% of deposited nitrogen undergoing dry deposition in the UK is mostly (64%) NH_3. There are no network measurements of dry deposition, though dominance of NH_3 has also been inferred from derived dry deposition fluxes obtained using concentration and meteorology measurements and modeled dry deposition velocities at UK monitoring sites (Flechard et al., 2011; Tang et al., 2009).

3.2. Influence of Emission Controls on $PM_{2.5}$ and Public Health

Figure 4 includes the decrease in modeled $PM_{2.5}$ resulting from control measures to meet current legislation (4b) and from adopting maximum technically feasible measures (4c). Decline in $PM_{2.5}$ in the CLE scenario is at most

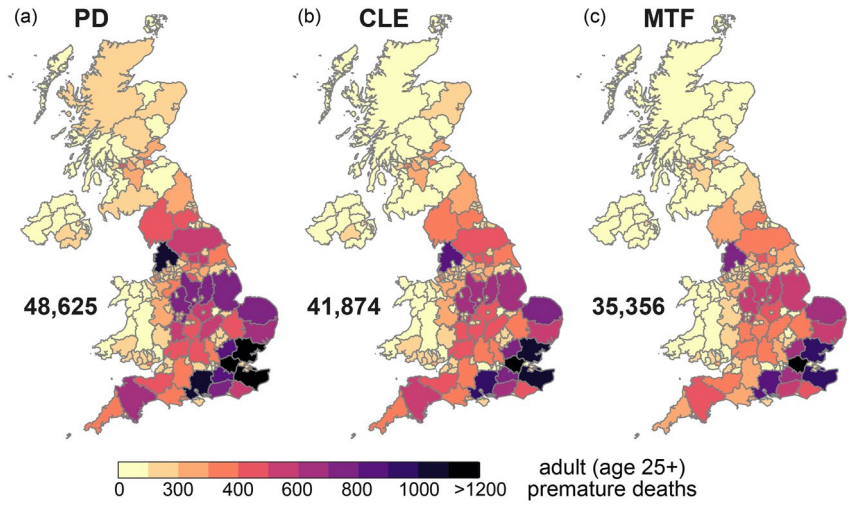

Figure 6. Present-day and future UK adult premature mortality attributable to exposure to $PM_{2.5}$. Maps are administrative area early deaths for the PD (2019) (a) and future (2030) with CLE (b) and MTF (c) emission controls. Inset values are premature mortality estimated with the hybrid eSCHIF-Fusion model detailed in Section 2.3 (see text for 95% confidence intervals).

2 μg m^{-3} and typically 0.9–1 μg m^{-3}. MTF measures achieve up to 5 μg m^{-3} decline in populated cities (London, Birmingham, Manchester, Leeds) and in locations with intensive industry (Welsh south coast) and large power plants (East Yorkshire). Greater decline in the MTF is due to combined decrease in point source emissions of SO_2, vehicular emissions of NO_x, and agricultural emissions of NH_3 (Figure 3). The largest decline is in April (3.7 μg m^{-3} UK mean) and the smallest is in summer months (1.1–1.5 μg m^{-3}). The percent UK grids in Figure 4a that exceed the WHO guideline declines from 79% in the PD to 58% in the CLE and 36% in the MTF. Most of the decline is over Northern Ireland and Scotland north and south of the Central Belt for the CLE and for the MTF this spreads to the rest of Scotland, all of Cornwall and most of Wales.

Figure 6 maps adult excess deaths attributable to exposure to $PM_{2.5}$ for all 3 scenarios in all UK administrative areas in the PD and by 2030 from adopting CLE or MTF measures. According to the cohort studies conducted to derive the curves used to estimate adult excess deaths, dominant health endpoints include ischemic heart disease, respiratory diseases, diabetes and cardiovascular disease (Brauer et al., 2022; Burnett et al., 2022). The eSCHIF portion of the hybrid curve (Equation 1; Figure 1) is applied to 85% of GEOS-Chem grids for the PD and all grids for the CLE and MTF scenarios. $PM_{2.5}$ in all administrative areas exceeds the 2.5 μg m^{-3} threshold for harm in the hybrid model (Figure 1). In the PD, UK annual premature mortality totals 48,625 (95% CI: 45,118–52,595) and on average 8% of premature adult deaths are attributable to exposure to $PM_{2.5}$. Greater London accounts for 10% of these (4,861; 95% CI: 4,549–5,247) and exceeds national totals for Scotland (3,673; 95% CI: 3,214–4,073), Wales (2,462; 95% CI: 2,270–2,660) and Northern Ireland (1,052; 95% CI: 934–1,156). Administrative areas other than Greater London that exceed a thousand excess deaths in the PD are Essex, Kent and Hampshire in southeast England and Lancashire in northwest England. Lancashire and Hampshire fall below 1,000 with CLE measures and all except Greater London fall below 1,000 with MTF measures.

Annual adult excess deaths for the UK in the PD obtained using GEMM (Figure 1) are 4,608 more than the hybrid model at 53,233 (95% CI: 38,526–67,539), due to higher RRs in GEMM for $PM_{2.5} > 7$ μg m^{-3} typical of populated cities in England (Figure 2a). The excess deaths we obtain for the UK in the PD with the hybrid model exceed previously published estimates of 28,969 for 2010 (Gowers et al., 2014) and 40,408 (95% CI: 30,867–45,050) for 2018 (Macintyre et al., 2023). These are both for adults ≥30 rather than ≥25 years old, but this difference has a small effect on burden of disease estimates, as premature mortality for the 25–30 age range is low (PHE, 2014). The curves used in past studies are compared to the hybrid model and GEMM in Figure 1. Incremental changes in risk used in those studies are on average 0.6% (Gowers et al., 2014) and 0.8% (Macintyre et al., 2023) per μg m^{-3} $PM_{2.5}$ or RRs of 1.06 (Gowers et al., 2014) and 1.08 (Macintyre et al., 2023) at 10 μg m^{-3}. The hybrid model change in risk per μg m^{-3} $PM_{2.5}$ ranges from almost 1% for $PM_{2.5} > 9.8$ μg m^{-3} (the Fusion portion of the curve) to 0.5% at 5–9.8 μg m^{-3} and 2.5% at 2.5–5 μg m^{-3}, due to variability in the eSCHIF curve gradient.

Decline in precursor emissions of $PM_{2.5}$ in the CLE results in a UK mean attributable fraction of 7% and total premature deaths of 41,874 (95% CI: 37,949–45,437) by 2030 or 6,751 avoided early deaths. In the MTF, premature deaths attributable to exposure to $PM_{2.5}$ averages 6% of all nonaccidental premature deaths and totals 35,356 (95% CI: 29,882–40,015) by 2030. This is 13,269 avoided deaths, representing 27% of PD premature deaths attributable to $PM_{2.5}$ and twice that achieved with current legislation. The GEMM curve also yields a factor of 2 benefit to public health from adopting best available technologies over what is currently legislated.

The elderly (65+) account for most (86%) early nonaccidental deaths in the GBD data and there will likely be 2.5 million more elderly people in the UK in 2030 than in 2020 (https://www.ons.gov.uk/peoplepopulationandcommunity/populationandmigration/populationprojections/bulletins/nationalpopulationprojections/2020basedinterim; last accessed 2 June 2023). We do not account for this increase in our 2030 premature mortality estimates. The effect would be to decrease the number of avoided early deaths resulting from emission controls. There is also recent epidemiological evidence for much greater RR than the hybrid curve (Figure 1) amongst the elderly exposed to $PM_{2.5}$ representative of concentrations in the UK. The causal inference study by Wu et al. (2020) used 16 years of US Medicare data to estimate an RR of at least 1.23 at 10 μg m^{-3} or on average a 2.3% decline in risk per μg m^{-3} decrease in $PM_{2.5}$ amongst the elderly for $PM_{2.5} \leq 12$ μg m^{-3}. This would substantially increase the number of premature deaths attributable to $PM_{2.5}$ in the PD, but also increase the number of avoided early deaths due to emission controls.

3.3. Harm of Nitrogen Deposition and Ambient NH_3 to Sensitive Habitats

GEOS-Chem nitrogen deposited to all UK land totals 253 Gg N in the PD. This is lower than values from higher-resolution models and derived data sets. GEOS-Chem deposition is 25 Gg N or 9% less than is simulated for 2017 with a 5 km resolution CTM (Tomlinson et al., 2021) and 57 Gg N less than gridded mean nitrogen deposition from the CBED data set (Section 2.4). According to GEOS-Chem, total deposited nitrogen is ∼40% of the emitted terrestrial and aviation anthropogenic nitrogen (601 Gg N, Figure 3), suggesting that more than half (∼60%) of the nitrogen emitted is exported offshore. As a result, decline in nitrogen deposition by 2030 is only about a third of the decrease in terrestrial and aviation nitrogen emissions from adopting emission controls. For CLE measures, nitrogen deposited to UK land decreases by 27 Gg N or 31% of the decline in terrestrial and aviation emissions of 88 Gg N (Figure 3). NH_x deposition increases in this scenario by 3 Gg N due to a 2% increase in NH_3 emissions. Decline in UK nitrogen deposition from MTF measures is 75 Gg N or 37% of the 205 Gg N decline in terrestrial and aviation emissions.

Nitrogen deposited to sensitive habitats in excess of critical loads (Figure 2a) is shown in Figure 7a for the PD (2019). Excess nitrogen covers 95% of sensitive habitats, totals 106 Gg N and averages 14 kg N ha^{-1}. The largest exceedances of >35 kg N ha^{-1} coincide with NH_3 emission hotspots associated with intensive livestock farming (Hellsten et al., 2008; Marais et al., 2021). By 2030, CLE controls decrease total nitrogen deposition to sensitive habitats by 6 Gg N and average exceedances by 1 kg N ha^{-1} (Figure 7b) compared to decline of 18 Gg N total and 2 kg N ha^{-1} average decline with MTF measures (Figure 7c). For both scenarios, decline in the extent of sensitive habitats exposed to excess nitrogen is modest at 4 percentage points for the CLE and 8 percentage points for the MTF. Almost all this decline is in northern Scotland. A similarly small decline (6 percentage points) is reported for a decade of emission controls from 2010 to 2019 (Rowe et al., 2022). Given that the decline in excess nitrogen deposition is <10% of the decline in emissions, an emissions reduction of at least 500 Gg N may be required to halve excess nitrogen deposition to 50 Gg N. This is ∼80% of present-day emissions or more than twice that feasible with best available measures.

The extent of UK ambient air with NH_3 concentration >1 μg m^{-3}, indicative of harm to bryophytes and lichens, is 73% in the PD. An increase in UK mean ambient NH_3 in the CLE of 8% increases UK area with $NH_3 > 1$ μg m^{-3} to 75%. This is due to concurrent increase in NH_3 emissions (Figure 3) and decline in the efficacy of the NH_3 acidic aerosol sink (sulfate + nitrate decline by 24%). MTF controls on both NH_3 and acidic aerosol precursor emissions of SO_2 and NO_x (Figure 3) cause decline in both NH_3 (by 13%) and sulfate + nitrate (by 46%), causing a modest decrease in the extent of $NH_3 > 1$ μg m^{-3} to 69%. As NH_3 is semi-volatile, its emissions depend on multiple environmental factors. A warmer world may, for example, substantially increase NH_3 emissions. One estimate suggests a 5°C warmer world increases global NH_3 emissions by 30%–70% (Sutton et al., 2013).

4. Conclusions

Particulate matter pollution even at the relatively low concentrations typical of the UK adversely affect human health and nitrogen pollution harms habitats sensitive to excess deposition and exposure to the phytotoxin

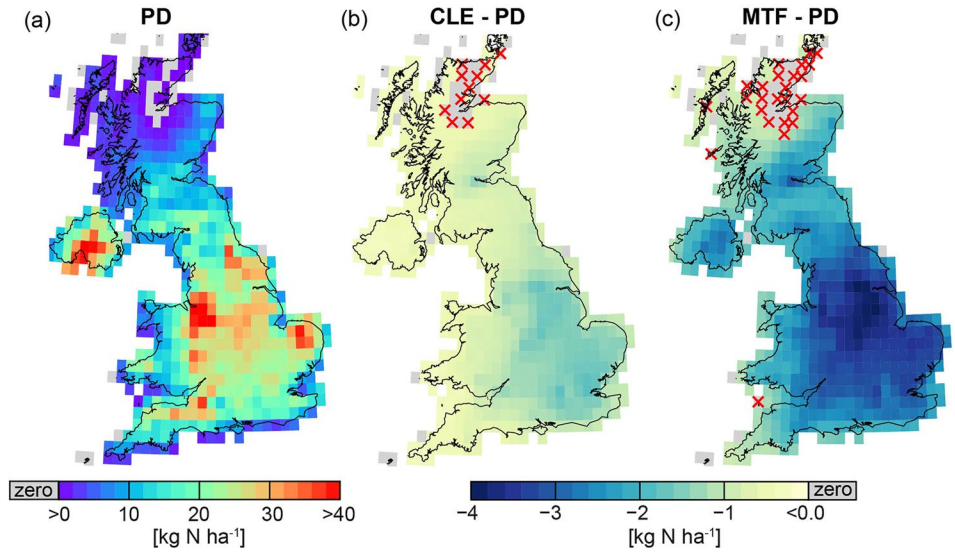

Figure 7. Impact of emission controls on excess nitrogen deposited to UK sensitive habitats. Maps are PD nitrogen deposition in excess of sensitive habitat critical loads obtained with CBED (a) and the change in excess nitrogen deposition resulting from CLE (b) and MTF (c) control measures from GEOS-Chem. All units are kg N (ha sensitive habitat)$^{-1}$ a^{-1}. Gray shaded grids are below critical loads and red crosses identify grids that fall below critical loads due to CLE (b) and MTF (c) controls.

ammonia (NH_3). We assess the potential health and ecosystem co-benefits that could be achieved in 2030 following legislative action or from adopting best available emission control measures using emissions projections, the GEOS-Chem model, high-spatial-resolution data sets, and up-to-date relationships between exposure and harm.

Legislative measures are most effective at targeting acidic aerosol (sulfate, nitrate) precursor emissions of sulfur dioxide (SO_2) and nitrogen oxides (NO_x), causing decline in fine particulate matter ($PM_{2.5}$) pollution and 6,751 avoided annual early deaths. The extent of the UK above the World Health Organization (WHO) 5 μg m^{-3} guideline for long-term exposure to ambient $PM_{2.5}$ also decreases from 79% to 58%. If instead best available measures are adopted, the number of avoided annual early deaths doubles to 13,269 and less than half (36%) the UK exceeds the WHO guideline.

The benefits to habitats are near-negligible for current legislation and modest for adoption of best available measures. Both NH_3 abundance and the amount of nitrogen deposited as NH_3 increase with current legislation, as controls on agricultural sources are ineffective at decreasing NH_3 emissions and loss of NH_3 to acidic aerosols declines. Adoption of best available measures decreases NH_3 emissions, as these target major agricultural sources, but these are also insufficient for improving ecosystem health. A far greater (at least 80%) decline in UK nitrogen emissions may be needed to halve harmful nitrogen deposition than the 34% achievable with best available measures.

Conflict of Interest

The authors declare no conflicts of interest relevant to this study.

Data Availability Statement

Data generated as part of this work and that are used, but not available for public access elsewhere, are available on the UCL Data Repository in NetCDF format. These include GEOS-Chem annual mean ambient $PM_{2.5}$ and NH_3 concentrations and annual total nitrogen deposition, attributable fraction and premature mortality generated with the eSCHIF-Fusion hybrid model, critical loads on the GEOS-Chem grid, UKCEH habitat maps at 1 km resolution, and CBED nitrogen deposition to forests and open vegetation at 5 km resolution (Marais et al., 2023). GEOS-Chem version 13.0.0 is preserved on Zenodo by The International GEOS-Chem User Community (2021).

Acknowledgments
The authors are grateful to Zbigniew Klimont for guidance on using the ECLIPSEv6b emissions data. This research has been supported by the European Research Council under the European Union's Horizon 2020 research and innovation program (through the Starting Grant awarded to Eloise A. Marais, UpTrop (Grant 851854)).

References

Alexandratos, N., & Bruinsma, J. (2012). World agriculture towards 2030/2050: The 2012 revision. ESA Working paper No. 12-03. Retrieved from https://www.fao.org/3/ap106e/ap106e.pdf

Amos, H. M., Jacob, D. J., Holmes, C. D., Fisher, J. A., Wang, Q., Yantosca, R. M., et al. (2012). Gas-particle partitioning of atmospheric $Hg_{(II)}$ and its effect on global mercury deposition. *Atmospheric Chemistry and Physics*, *12*(1), 591–603. https://doi.org/10.5194/acp-12-591-2012

Backes, A. M., Aulinger, A., Bieser, J., Matthias, V., & Quante, M. (2016). Ammonia emissions in Europe, part II: How ammonia emission abatement strategies affect secondary aerosols. *Atmospheric Environment*, *126*, 153–161. https://doi.org/10.1016/j.atmosenv.2015.11.039

Bobbink, R., Hornung, M., & Roelofs, J. G. M. (1998). The effects of air-borne nitrogen pollutants on species diversity in natural and semi-natural European vegetation. *Journal of Ecology*, *86*(5), 717–738. https://doi.org/10.1046/j.1365-2745.1998.8650717.x

Bobbink, R., Loran, C., & Tomassen, H. (2022). *Review and revision of empirical critical loads of nitrogen for Europe* (p. 358). German Environment Agency (UBA). Retrieved from https://www.umweltbundesamt.de/sites/default/files/medien/1410/publikationen/2022-10-12_texte_110-2022_review_revision_empirical_critical_loads.pdf

Bouwman, A. F., Lee, D. S., Asman, W. A. H., Dentener, F. J., Van Der Hoek, K. W., & Olivier, J. G. J. (1997). A global high-resolution emission inventory for ammonia. *Global Biogeochemical Cycles*, *11*(4), 561–587. https://doi.org/10.1029/97gb02266

Brauer, M., Brook, J. R., Christidis, T., Chu, Y., Crouse, D. L., Erickson, A., et al. (2022). *Mortality–air pollution associations in low exposure environments (MAPLE): Phase 2*. HEI. Retrieved from https://www.ncbi.nlm.nih.gov/pmc/articles/PMC9556709/pdf/hei-2022-212.pdf

Burnett, R., Chen, H., Szyszkowicz, M., Fann, N., Hubbell, B., Pope, C. A., et al. (2018). Global estimates of mortality associated with long-term exposure to outdoor fine particulate matter. *Proceedings of the National Academy of Sciences of the United States of America*, *115*(38), 9592–9597. https://doi.org/10.1073/pnas.1803222115

Burnett, R. T., Spadaro, J. V., Garcia, G. R., & Pope, C. A. (2022). Designing health impact functions to assess marginal changes in outdoor fine particulate matter. *Environmental Research*, *204*, 112245. https://doi.org/10.1016/j.envres.2021.112245

Cape, J. N., van der Eerden, L. J., Sheppard, L. J., Leith, I. D., & Sutton, M. A. (2009). Evidence for changing the critical level for ammonia. *Environmental Pollution*, *157*(3), 1033–1037. https://doi.org/10.1016/j.envpol.2008.09.049

Chin, M., Ginoux, P., Kinne, S., Torres, O., Holben, B. N., Duncan, B. N., et al. (2002). Tropospheric aerosol optical thickness from the GOCART model and comparisons with satellite and sun photometer measurements. *Journal of the Atmospheric Sciences*, *59*(3), 461–483. https://doi.org/10.1175/1520-0469(2002)059<0461:Taotft>2.0.Co;2

Churchill, S., Richmond, B., MacCarthy, J., Broomfield, M., Brown, P., Del Vento, S., et al. (2022). UK informative inventory report (1990 to 2020). Retrieved from https://uk-air.defra.gov.uk/assets/documents/reports/cat09/2203151456_GB_IIR_2022_Submission_v1.pdf

Cohen, A. J., Brauer, M., Burnett, R., Anderson, H. R., Frostad, J., Estep, K., et al. (2017). Estimates and 25-year trends of the global burden of disease attributable to ambient air pollution: An analysis of data from the Global Burden of Diseases Study 2015. *The Lancet*, *389*(10082), 1907–1918. https://doi.org/10.1016/s0140-6736(17)30505-6

Conolly, C., Vincent, K., Sanocka, A., Richie, S., Knight, D., Donovan, B., et al. (2021). UKEAP 2021 annual report. Retrieved from https://uk-air.defra.gov.uk/assets/documents/reports/cat09/2209290921_2021UKEAP_EA_final.pdf

Cooke, W. F., Liousse, C., Cachier, H., & Feichter, J. (1999). Construction of a 1°×1° fossil fuel emission data set for carbonaceous aerosol and implementation and radiative impact in the ECHAM4 model. *Journal of Geophysical Research*, *104*(D18), 22137–22162. https://doi.org/10.1029/1999jd900187

DEFRA. (2018). Code of good agricultural practice (COGAP) for reducing ammonia emissions. Retrieved from https://assets.publishing.service.gov.uk/government/uploads/system/uploads/attachment_data/file/729646/code-good-agricultural-practice-ammonia.pdf

Di, Q., Wang, Y., Zanobetti, A., Wang, Y., Koutrakis, P., Choirat, C., et al. (2017). Air pollution and mortality in the medicare population. *New England Journal of Medicine*, *376*(26), 2513–2522. https://doi.org/10.1056/NEJMoa1702747

Dise, N. B., Ashmore, M., Belyazid, S., Bleeker, A., Bobbink, R., de Vries, W., et al. (2011). Nitrogen as a threat to European terrestrial biodiversity. In A. Bleeker, B. Grizzetti, C. M. Howard, G. Billen, H. vanGrinsven, J. W. Erisman, et al. (Eds.), *The European nitrogen assessment: Sources, effects and policy perspectives* (pp. 463–494). Cambridge University Press. https://doi.org/10.1017/CBO9780511976988.023

Dore, A. J., Choularton, T. W., Brown, R., & Blackall, R. M. (1992). Orographic rainfall enhancement in the mountains of the Lake District and Snowdonia. *Atmospheric Environment, Part A: General Topics*, *26*(3), 357–371. https://doi.org/10.1016/0960-1686(92)90322-c

Fairlie, T. D., Jacob, D. J., & Park, R. J. (2007). The impact of transpacific transport of mineral dust in the United States. *Atmospheric Environment*, *41*(6), 1251–1266. https://doi.org/10.1016/j.atmosenv.2006.09.048

Flechard, C. R., Nemitz, E., Smith, R. I., Fowler, D., Vermeulen, A. T., Bleeker, A., et al. (2011). Dry deposition of reactive nitrogen to European ecosystems: A comparison of inferential models across the NitroEurope network. *Atmospheric Chemistry and Physics*, *11*(6), 2703–2728. https://doi.org/10.5194/acp-11-2703-2011

Fountoukis, C., & Nenes, A. (2007). ISORROPIA II: A computationally efficient thermodynamic equilibrium model for K^+-Ca_2^+-Mg_2^+-NH_4^+-Na^+-SO_4^{2-}-NO_3^--Cl^--H_2O aerosols. *Atmospheric Chemistry and Physics*, *7*(17), 4639–4659. https://doi.org/10.5194/acp-7-4639-2007

Fowler, D., Cape, J. N., Leith, I. D., Choularton, T. W., Gay, M. J., & Jones, A. (1988). The influence of altitude on rainfall composition at Great Dun Fell. *Atmospheric Environment*, *22*(7), 1355–1362. https://doi.org/10.1016/0004-6981(88)90160-6

Freeman, S., Lee, D. S., Lim, L. L., Skowron, A., & De León, R. R. (2018). Trading off aircraft fuel burn and NO_x emissions for optimal climate policy. *Environmental Science & Technology*, *52*(5), 2498–2505. https://doi.org/10.1021/acs.est.7b05719

Fricko, O., Havlik, P., Rogelj, J., Klimont, Z., Gusti, M., Johnson, N., et al. (2017). The marker quantification of the Shared Socioeconomic Pathway 2: A middle-of-the-road scenario for the 21st century. *Global Environmental Change*, *42*, 251–267. https://doi.org/10.1016/j.gloenvcha.2016.06.004

Giannakis, E., Kushta, J., Bruggeman, A., & Lelieveld, J. (2019). Costs and benefits of agricultural ammonia emission abatement options for compliance with European air quality regulations. *Environmental Sciences Europe*, *31*(1), 93. https://doi.org/10.1186/s12302-019-0275-0

Gowers, A. M., Miller, B. G., & Stedman, J. R. (2014). Estimating local mortality burdens associated with particulate air pollution. Retrieved from https://www.gov.uk/government/publications/estimating-local-mortality-burdens-associated-with-particulate-air-pollution

Hall, J., Curtis, C., Dore, T., & Smith, R. (2015). Methods for the calculation of critical loads and their exceedances in the UK. Retrieved from http://www.cldm.ceh.ac.uk/content/methods-calculation-critical-loads-and-their-exceedances-uk

Hellsten, S., Dragosits, U., Place, C. J., Vieno, M., Dore, A. J., Misselbrook, T. H., et al. (2008). Modelling the spatial distribution of ammonia emissions in the UK. *Environmental Pollution*, *154*(3), 370–379. https://doi.org/10.1016/j.envpol.2008.02.017

Henneman, L. R. F., Rafaj, P., Annegarn, H. J., & Klausbruckner, C. (2016). Assessing emissions levels and costs associated with climate and air pollution policies in South Africa. *Energy Policy*, *89*, 160–170. https://doi.org/10.1016/j.enpol.2015.11.026

Hertel, O., Skjøth, C. A., Reis, S., Bleeker, A., Harrison, R. M., Cape, J. N., et al. (2012). Governing processes for reactive nitrogen compounds in the European atmosphere. *Biogeosciences*, *9*(12), 4921–4954. https://doi.org/10.5194/bg-9-4921-2012

IMO. (2019). Nitrogen oxides (NO_x)—Regulation 13. Retrieved from: https://www.imo.org/en/OurWork/Environment/Pages/Nitrogen-oxides-(NOx)-%E2%80%93-Regulation-13.aspx

Jaeglé, L., Quinn, P. K., Bates, T. S., Alexander, B., & Lin, J. T. (2011). Global distribution of sea salt aerosols: New constraints from in situ and remote sensing observations. *Atmospheric Chemistry and Physics*, *11*(7), 3137–3157. https://doi.org/10.5194/acp-11-3137-2011

Kelleghan, D. B., Tang, Y. S., Rowe, E. C., Jones, L., Curran, T. P., McHugh, K., et al. (2021). National ecosystem monitoring network (NEMN)-design: Monitoring air pollution impacts across sensitive ecosystems. Retrieved from https://www.epa.ie/publications/monitoring--assessment/air/national-ecosystems-monitoring-network/NEMN-Design_v04-FINAL-(003).pdf

Keller, C. A., Long, M. S., Yantosca, R. M., Da Silva, A. M., Pawson, S., & Jacob, D. J. (2014). HEMCO v1.0: A versatile, ESMF-compliant component for calculating emissions in atmospheric models. *Geoscientific Model Development*, *7*(4), 1409–1417. https://doi.org/10.5194/gmd-7-1409-2014

Kelly, J. M., Marais, E. A., Lu, G., Obszynska, J., Mace, M., White, J., & Leigh, R. J. (2023). Diagnosing domestic and transboundary sources of fine particulate matter ($PM_{2.5}$) in UK cities using. *GEOS-Chem, City and Environment Interactions*, *18*, 100100. https://doi.org/10.1016/j.cacint.2023.100100

Klimont, Z., & Brink, C. (2004). Modelling of emissions of air pollutants and greenhouse gases from agricultural sources in Europe. Retrieved from https://pure.iiasa.ac.at/id/eprint/7400/1/IR-04-048.pdf

Krupa, S. V. (2003). Effects of atmospheric ammonia (NH_3) on terrestrial vegetation: A review. *Environmental Pollution*, *124*(2), 179–221. https://doi.org/10.1016/s0269-7491(02)00434-7

Liu, H. Y., Jacob, D. J., Bey, I., & Yantosca, R. M. (2001). Constraints from ^{210}Pb and ^{7}Be on wet deposition and transport in a global three-dimensional chemical tracer model driven by assimilated meteorological fields. *Journal of Geophysical Research*, *106*(D11), 12109–12128. https://doi.org/10.1029/2000jd900839

Luo, G., Yu, F., & Moch, J. M. (2020). Further improvement of wet process treatments in GEOS-Chem v12.6.0: Impact on global distributions of aerosols and aerosol precursors. *Geoscientific Model Development*, *13*(6), 2879–2903. https://doi.org/10.5194/gmd-13-2879-2020

Macintyre, H. L., Mitsakou, C., Vieno, M., Heal, M. R., Heaviside, C., & Exley, K. S. (2023). Impacts of emissions policies on future UK mortality burdens associated with air pollution. *Environment International*, *174*, 107862. https://doi.org/10.1016/j.envint.2023.107862

Marais, E. A., Kelly, J. M., Obszynska, J., Mace, M., White, J., & Leigh, R. J. (2022). GEOS-Chem model output for diagnosing sources of fine particles ($PM_{2.5}$) in UK cities [Dataset]. https://doi.org/10.5522/04/20305401

Marais, E. A., Kelly, J. M., Vohra, K., Rowe, E. C., & Hina, N. (2023). GEOS-Chem model output used to assess UK public and ecosystem health benefits of emission controls [Dataset]. University College London. https://doi.org/10.5522/04/23540079

Marais, E. A., Pandey, A. K., Van Damme, M., Clarisse, L., Coheur, P. F., Shephard, M. W., et al. (2021). UK ammonia emissions estimated with satellite observations and GEOS-Chem. *Journal of Geophysical Research-Atmospheres*, *126*(18), e2021JD035237. https://doi.org/10.1029/2021jd035237

Meng, J., Martin, R. V., Ginoux, P., Hammer, M., Sulprizio, M. P., Ridley, D. A., & van Donkelaar, A. (2021). Grid-independent high-resolution dust emissions (v1.0) for chemical transport models: Application to GEOS-Chem (12.5.0). *Geoscientific Model Development*, *14*(7), 4249–4260. https://doi.org/10.5194/gmd-14-4249-2021

Murray, L. T., Jacob, D. J., Logan, J. A., Hudman, R. C., & Koshak, W. J. (2012). Optimized regional and interannual variability of lightning in a global chemical transport model constrained by LIS/OTD satellite data. *Journal of Geophysical Research*, *117*(D20), D20307. https://doi.org/10.1029/2012jd017934

Neelam, M., Bindlish, R., O'Neill, P., Huffman, G. J., Reichle, R., Chan, S., & Colliander, A. (2021). Evaluation of GEOS precipitation flagging for SMAP soil moisture retrieval accuracy. *Journal of Hydrometeorology*. https://doi.org/10.1175/jhm-d-20-0038.1

Office of the European Union. (2016a). Directive (EU) 2016/2284 of the European parliament and of the council. Retrieved from https://eur-lex.europa.eu/legal-content/EN/TXT/PDF/?uri=CELEX:32016L2284&from=EN

Office of the European Union. (2016b). Directive (EU) 2016/802 of the European Parliament and of the Council of 11 May 2016 relating to a reduction in the sulphur content of certain liquid fuels. Retrieved from https://eur-lex.europa.eu/legal-content/EN/TXT/PDF/?uri=CELEX:32016L0802&rid=1

Pai, S. J., Heald, C. L., Pierce, J. R., Farina, S. C., Marais, E. A., Jimenez, J. L., et al. (2020). An evaluation of global organic aerosol schemes using airborne observations. *Atmospheric Chemistry and Physics*, *20*(5), 2637–2665. https://doi.org/10.5194/acp-20-2637-2020

Park, R. J., Jacob, D. J., Field, B. D., Yantosca, R. M., & Chin, M. (2004). Natural and transboundary pollution influences on sulfate-nitrate-ammonium aerosols in the United States: Implications for policy. *Journal of Geophysical Research*, *109*(D15), 20. https://doi.org/10.1029/2003jd004473

Paulot, F., Jacob, D. J., Pinder, R. W., Bash, J. O., Travis, K., & Henze, D. K. (2014). Ammonia emissions in the United States, European Union, and China derived by high-resolution inversion of ammonium wet deposition data: Interpretation with a new agricultural emissions inventory (MASAGE_NH_3). *Journal of Geophysical Research: Atmospheres*, *119*(7), 4343–4364. https://doi.org/10.1002/2013jd021130

PHE. (2014). Estimating local mortality burdens associated with particulate air pollution. Retrieved from https://assets.publishing.service.gov.uk/government/uploads/system/uploads/attachment_data/file/332854/PHE_CRCE_010.pdf

Phoenix, G. K., Emmett, B. A., Britton, A. J., Caporn, S. J. M., Dise, N. B., Helliwell, R., et al. (2012). Impacts of atmospheric nitrogen deposition: Responses of multiple plant and soil parameters across contrasting ecosystems in long-term field experiments. *Global Change Biology*, *18*(4), 1197–1215. https://doi.org/10.1111/j.1365-2486.2011.02590.x

Pope, R. J., Kelly, R., Marais, E. A., Graham, A. M., Wilson, C., Harrison, J. J., et al. (2022). Exploiting satellite measurements to explore uncertainties in UK bottom-up NO_x emission estimates. *Atmospheric Chemistry and Physics*, *22*(7), 4323–4338. https://doi.org/10.5194/acp-22-4323-2022

Potts, D. A., Marais, E. A., Boesch, H., Pope, R. J., Lee, J., Drysdale, W., et al. (2021). Diagnosing air quality changes in the UK during the COVID-19 lockdown using TROPOMI and GEOS-Chem. *Environmental Research Letters*, *16*(5), 054031. https://doi.org/10.1088/1748-9326/abde5d

Richmond, B., Misra, A., Brown, P., Karagianni, E., Murrells, T., Pang, Y., et al. (2020). *UK informative inventory report (1990 to 2018)*. Ricardo Energy & Environment. Retrieved from https://uk-air.defra.gov.uk/assets/documents/reports/cat07/2003131327_GB_IIR_2020_v1.0.pdf

Riddick, S. N., Dragosits, U., Blackall, T. D., Daunt, F., Wanless, S., & Sutton, M. A. (2012). The global distribution of ammonia emissions from seabird colonies. *Atmospheric Environment*, *55*, 319–327. https://doi.org/10.1016/j.atmosenv.2012.02.052

Rowe, E., & Hina, N. (2023). *Empirical critical loads for nutrient nitrogen: Defining mapping values for UK habitats*. Unpublished report to Defra on National Focal Centre project. UKCEH.

Rowe, E. C., Hina, N. S., Carnell, E., Vieno, M., Levy, P., Raine, B., et al. (2022). *Trends Report 2022: Trends in critical load and critical level exceedances in the UK*. UKCEH. Retrieved from https://uk-air.defra.gov.uk/library/reports?report_id=1087

Sala, O. E., Stuart Chapin, F., III., Armesto, J. J., Berlow, E., Bloomfield, J., Dirzo, R., et al. (2000). Global biodiversity scenarios for the year 2100. *Science*, *287*(5459), 1770–1774. https://doi.org/10.1126/science.287.5459.1770

Skowron, A., Lee, D. S., De León, R. R., Lim, L. L., & Owen, B. (2021). Greater fuel efficiency is potentially preferable to reducing NO_x emissions for aviation's climate impacts. *Nature Communications*, *12*(1), 564. https://doi.org/10.1038/s41467-020-20771-3

Stohl, A., Aamaas, B., Amann, M., Baker, L. H., Bellouin, N., Berntsen, T. K., et al. (2015). Evaluating the climate and air quality impacts of short-lived pollutants. *Atmospheric Chemistry and Physics*, *15*(18), 10529–10566. https://doi.org/10.5194/acp-15-10529-2015

Strak, M., Weinmayr, G., Rodopoulou, S., Chen, J., de Hoogh, K., Andersen, Z. J., et al. (2021). Long term exposure to low level air pollution and mortality in eight European cohorts within the ELAPSE project: Pooled analysis. *The BMJ*, n1904. https://doi.org/10.1136/bmj.n1904

Sutton, M. A., Reis, S., Riddick, S. N., Dragosits, U., Nemitz, E., Theobald, M. R., et al. (2013). Towards a climate-dependent paradigm of ammonia emission and deposition. *Philosophical Transactions of the Royal Society B: Biological Sciences*, *368*(1621), 20130166. https://doi.org/10.1098/rstb.2013.0166

Sutton, M. A., van Dijk, N., Levy, P. E., Jones, M. R., Leith, I. D., Sheppard, L. J., et al. (2020). Alkaline air: Changing perspectives on nitrogen and air pollution in an ammonia-rich world. *Philosophical Transactions of the Royal Society A: Mathematical, Physical & Engineering Sciences*, *378*(2183), 20190315. https://doi.org/10.1098/rsta.2019.0315

Tang, Y. S., Braban, C. F., Dragosits, U., Simmons, I., Leaver, D., van Dijk, N., et al. (2018). Acid gases and aerosol measurements in the UK (1999–2015): Regional distributions and trends. *Atmospheric Chemistry and Physics*, *18*(22), 16293–16324. https://doi.org/10.5194/acp-18-16293-2018

Tang, Y. S., Simmons, I., van Dijk, N., Di Marco, C., Nemitz, E., Dämmgen, U., et al. (2009). European scale application of atmospheric reactive nitrogen measurements in a low-cost approach to infer dry deposition fluxes. *Agriculture, Ecosystems & Environment*, *133*(3–4), 183–195. https://doi.org/10.1016/j.agee.2009.04.027

The International GEOS-Chem User Community. (2021). GEOS-Chem version 13.0.0 [Software]. Zenodo. https://doi.org/10.5281/zenodo.4618180

Tomlinson, S. J., Carnell, E. J., Dore, A. J., & Dragosits, U. (2021). Nitrogen deposition in the UK at 1 km resolution from 1990 to 2017. *Earth System Science Data*, *13*(10), 4677–4692. https://doi.org/10.5194/essd-13-4677-2021

Travis, K. R., Jacob, D. J., Fisher, J. A., Kim, P. S., Marais, E. A., Zhu, L., et al. (2016). Why do models overestimate surface ozone in the Southeast United States? *Atmospheric Chemistry and Physics*, *16*(21), 13561–13577. https://doi.org/10.5194/acp-16-13561-2016

UK. (2018). The national emission ceilings regulations 2018 (No. 129). Retrieved from https://www.legislation.gov.uk/uksi/2018/129/made/data.pdf

van Herk, C. M., Mathijssen-Spiekman, E. A. M., & de Zwart, D. (2007). Long distance nitrogen air pollution effects on lichens in Europe. *The Lichenologist*, *35*(4), 347–359. https://doi.org/10.1016/s0024-2829(03)00036-7

van Vuuren, D. P., Stehfest, E., Gernaat, D. E. H. J., Doelman, J. C., van den Berg, M., Harmsen, M., et al. (2017). Energy, land-use and greenhouse gas emissions trajectories under a green growth paradigm. *Global Environmental Change*, *42*, 237–250. https://doi.org/10.1016/j.gloenvcha.2016.05.008

Vieno, M., Heal, M. R., Williams, M. L., Carnell, E. J., Nemitz, E., Stedman, J. R., & Reis, S. (2016). The sensitivities of emissions reductions for the mitigation of UK $PM_{2.5}$. *Atmospheric Chemistry and Physics*, *16*(1), 265–276. https://doi.org/10.5194/acp-16-265-2016

Vohra, K., Vodonos, A., Schwartz, J., Marais, E. A., Sulprizio, M. P., & Mickley, L. J. (2021). Global mortality from outdoor fine particle pollution generated by fossil fuel combustion: Results from GEOS-Chem. *Environmental Research*, *195*, 110754. https://doi.org/10.1016/j.envres.2021.110754

Weichenthal, S., Pinault, L., Christidis, T., Burnett, R. T., Brook, J. R., Chu, Y., et al. (2022). How low can you go? Air pollution affects mortality at very low levels. *Science Advances*, *8*(39). https://doi.org/10.1126/sciadv.abo3381

Weng, H., Lin, J., Martin, R., Millet, D. B., Jaeglé, L., Ridley, D., et al. (2020). Global high-resolution emissions of soil NO_x, sea salt aerosols, and biogenic volatile organic compounds. *Scientific Data*, *7*(1), 148. https://doi.org/10.1038/s41597-020-0488-5

Wesely, M. L. (1989). Parameterization of surface resistances to gaseous dry deposition in regional-scale numerical models. *Atmospheric Environment*, *23*(6), 1293–1304. https://doi.org/10.1016/0004-6981(89)90153-4

WHO. (2021). WHO global air quality guidelines: Particulate matter ($PM_{2.5}$ and PM_{10}), ozone, nitrogen dioxide, sulfur dioxide and carbon monoxide. Retrieved from https://apps.who.int/iris/handle/10665/345329

Woodward, H., Oxley, T., Rowe, E. C., Dore, A. J., & ApSimon, H. (2022). An exceedance score for the assessment of the impact of nitrogen deposition on habitats in the UK. *Environmental Modelling & Software*, *150*, 105355. https://doi.org/10.1016/j.envsoft.2022.105355

Wu, X., Braun, D., Schwartz, J., Kioumourtzoglou, M. A., & Dominici, F. (2020). Evaluating the impact of long-term exposure to fine particulate matter on mortality among the elderly. *Science Advances*, *6*(29). https://doi.org/10.1126/sciadv.aba5692